Microfluidic manufacturing of phospholipid nanoparticles: stability, encapsulation efficacy, and drug release

Mariana Guimarães Sá Correia[1], Maria L. Briuglia[2], Fabio Niosi[3], Dimitrios A. Lamprou[1, 2, 4*]

[1]Strathclyde Institute of Pharmacy and Biomedical Sciences (SIPBS), University of Strathclyde, 161 Cathedral Street, G4 0RE Glasgow, United Kingdom.

[2]National EPSRC Centre for Innovative Manufacturing in Continuous Manufacturing and Crystallisation (CMAC), University of Strathclyde, Technology and Innovation Centre, 99 George Street, G1 1RD Glasgow, United Kingdom.

[3]School of Chemistry, Trinity College Dublin, College Green, Dublin 2, Ireland Centre for Research on Adaptive Nanostructures and Nanodevices (CRANN), Trinity College Dublin, College Green, Dublin 2, Ireland.

[4]New Address: Medway School of Pharmacy, University Kent, Medway Campus, Anson Building, Central Avenue, Chatham Maritime, Chatham, ME4 4TB Kent, United Kingdom.

*Corresponding author. E-mail Address: D.Lamprou@kent.ac.uk. Tel.: +44(0) 1634 20 2947

Abstract

Liposomes have been the centre of attention in research due to their potential to act as drug delivery systems. Although its versatility and manufacturing processes are still not scalable and reproducible. In this study, the microfluidic method for liposomes preparation is presented. DMPC and DSPC liposomes containing two different lipid/cholesterol ratios (1:1 and 2:1) are prepared. Results from this preparation process were compared with the film hydration method in order to understand benefits and drawbacks of microfluidics. Liposomes characterisation was evaluated through stability studies, encapsulation efficacy and drug release profiles of hydrophilic and lipophilic compounds. Stability tests were performed during 3 weeks and the liposomes properties of the most stable formulations were determined using Infrared

Microscopy and Atomic Force Microscopy. Microfluidic allows loading of drugs and assembly in a quick single step and the chosen flow ratio for liposomes formulation plays a fundamental role for particle sizes. One hydrophilic and one lipophilic compound were incorporated showing how formulation and physic-chemical characteristics can influence the drug release profile.

Keywords: liposomes, microfluidics, encapsulation efficacy, controlled release.

1. Introduction

Liposomes are lipid structures that can be self-assembled naturally or prepared with natural or synthetic lipids [Immordino et al., 2006; Yadav et al., 2011]. These molecules present an amphipathic environment, which allows hydrophobic and hydrophilic drugs incorporation, thus providing an excellent structure for drug delivery systems [Immordino et al., 2006; Pattni et al., 2015]. The stability of the liposomal product depends on chemical, physical, and biological properties. Changes can occur during storage and modify important features correlated to the drug delivery process. Chemical transformations for example can influence in vivo fate of the liposome by affecting its loading and releasing properties [Heurtault, 2003].

Liposome production aims to achieve predictable and reproducible particle size distributions [Kreuter, 1994]. Commonly used methods for liposome formulation include hydration of lipids in aqueous buffer, freeze-thaw cycling, film hydration, reversed phase evaporation, normal phase integration, detergent depletion, and pH adjustment [Jahn et al., 2007]. All of these are conducted through the mixing of bulk phases. Traditional bulk methods of preparing liposomes are often characterised by heterogeneous and poorly controlled chemical and/or mechanical conditions that often result in liposomes poly-disperse in size and lamellarity [Jahn et al., 2004, 2007].

Due to these difficulties, microfluidics techniques overcome reproducibility problems. They work with small volume of fluids (10^{-9} to 10^{-8} litres) within channels with dimensions of 10 to 100 micrometres [Whitesides, 2006]. Many advantages come with usage of these techniques, such as more thoughtful use of sample and reagent resources, possibility to carry out separations and detections with higher resolution and sensitivity, lower cost of the whole procedure, quicker analysis, and small footprints for the analytical devices [Squires and Quake, 2005; Whitesides, 2006]. Microfluidic systems step up in the area of drug delivery with promising features that allow control of particle size and stability of the final liposome product, during preparation with simple steps like applying different flow rate ratios (FRR) and total flow rate (TFR); Fig. 1.

One of the aims of this study is to compare quality and properties of microfluidics formulations with liposomes generated through the hydration method in a previous study from our group [Briuglia et al., 2015]. In this current study, we changed the lipid:cholesterol ratio depending on the different applied FRR and TFR. The best formulation was chosen, and Atomic Force microscopy (AFM) studies were performed in order to evaluate liposome morphology. Finally, drug delivery studies with the same hydrophobic and hydrophilic drugs used by Briuglia et al. were encapsulated in order to investigate possible analogies or differences in terms of drug release. In our previous study, the most stable liposome composition was 2:1 as lipid:cholesterol ratio. The encapsulation efficacy was of 90% for atenolol (AT) and 88 % for quinine (Q) and the release profiles showed faster results for the hydrophilic molecule. In this paper, we compared hydration method with microfluidics formulation, and underline the benefits of microfluidics for industrial liposomes production.

2. Materials and Methods

2.1. Materials

The synthetic 1,2-dimyristoyl-sn-glycero-3-phosphocholine (DMPC) (≥98%) and 1,2-distearoyl-sn-glycero-3- phosphocholine (DSPC) (≥98%) were a gift from Lipoid GmbH (Fig. 2). Cholesterol (CH) (≥99%), Tablets of phosphate-buffered saline (PBS, pH 7.4), atenolol (AT) (≥98%) and quinine (Q) (≥98%) were all obtained from Sigma-Aldrich.

2.2. Preparation of liposomes

Liposomes were prepared using a microfluidic micro-mixer, which through hydrodynamic flow enables nano precipitation of lipids. The system known as NanoAssemblr^{TM} (Benchtop, Precision NanoSystems Inc., Vancouver, Canada) contains a microfluidic cartridge (52 mm thick and 36 mm height with moulded channels of 300 µm in width and 130 µm in height with staggered herringbone structures). The Nanoassemblr mixing chips have two stream inlets that merge into a micro-channel (Fig. 1). The two inlets used correspond to the lipid mixtures, which were dissolved in an organic solvent (ethanol), and the aqueous buffer (PBS, pH 7.4). Both fluids were pumped into the two inlets of the microfluidic micro-mixer using disposable syringes. The staggered herringbone structure of the micro-mixer enhances the advection and diffusion of the fluids flowing through the micro-channel [Belliveau et al., 2012]. By inducing rotational flow, the fluid streams get wrapped around each other, allowing the introduction of chaotic flow profile, that results in faster mixing of fluids [Belliveau et al., 2012]. The NanoAssemblr^{TM} allowed the control of TFR (1, 6, 20 mL.ml^{-1}) and the FRR (1:1, 3:1 and 5:1 ratio of the aqueous: solvent) between the two inlet streams through computerised syringe pumps. An increase at FRR (e.g. 1:1 to 1:3 aqueous/ethanol) was reported to cause a decrease of mean size of liposomes along with the increase of polydispersity index (PDI) [Kastner et al., 2014, 2015]. Additionally, TFR did not show significant effects on the liposome size, zeta (ζ) potential and polydispersity index (PDI) [Kastner et al., 2014, 2015].

Two different ratios of lipid/cholesterol were used in the experiment, 1:1 and 2:1. For the encapsulation studies AT and Q were dissolved in PBS (at a concentration of 10 mg ml^{-1} for AT and 0.3 mg ml^{-1} Q).

2.3 Stability Studies

The stability tests were conducted for three weeks after the liposome formulations. The samples were divided into two batches and stored in controlled temperature rooms at 4°C and 37 °C. Size, PDI and ζ-potential were measured three times every week. Particles morphology was investigated using Atomic Force Microscopy (AFM) at week 0 for the four most stable formulations.

2.4 Liposomes Physicochemical Characterisation

2.4.1 Dynamic Light Scattering (DLS)

The size distribution (mean diameter and PDI) of the liposomes was measured by dynamic light scattering (DLS) on a Zetasizer Nano-ZS (Malvern Instruments Ltd., UK), which enabled to obtain the mass distribution of particle size as well as the electrophoretic mobility. Measurements were made at 20 °C with a fixed angle of 137 ° in a dilution of 1/100 using PBS pH 7.4. Sizes quoted are the z-average mean (dz) for the liposomal hydrodynamic diameter (nm). Moreover, the same equipment was used to measure the ζ-potential for all formulations.

2.4.2 Fourier Transform Infrared Spectroscopy (FTIR)

The characterisation of the liposome formulations using FTIR was performed in order to understand if the CH interaction with phospholipids was changed by the microfluidic method. The pellets formulations were scanned in an inert atmosphere over a wave number range of

3000-1500 cm^{-1} over 128 scans at a resolution of 4 cm^{-1} and an interval of 1 cm^{-1}. All FT-IR spectra were recorder on BRUKER tensor II FT-IR Spectrometer and the background was subtracted from each spectrum.

2.4.3 Atomic Force Microscopy (AFM)

A volume of 5 µl from each formulation was placed on a freshly cleaved mica surface (1.5 cm x 1.5 cm; G250-2 Mica sheets 1" x 1" x 0.006"; Agar Scientific Ltd., Essex, UK). The sample was then air-dried for ~30 min and imaged at once by scanning the mica surface in air under ambient conditions using a Bruker MultiMode 8 Scanning Probe Microscope (Digital Instruments, Santa Barbara, CA, USA) operated on Peak Force QNM mode. The AFM measurements were obtained using ScanAsyst-air probes; the spring constant was calibrated by thermal tune (Nominal 0.4 N m^{-1}) and the deflection sensitivity calibrated using a silica wafer. AFM scans were acquired at a resolution of 512 x 512 pixels at scan rate of 1 Hz, and produced topographic images of the samples in which the brightness of features increases as a function of height. AFM images were collected from random spot surface sampling.

2.5 Dialysis dynamic experiment

Dynamic dialysis is one of the most commonly used methods for the determination of release kinetics from nanoparticles [Modi and Anderson, 2013]. Prior to the addition of the mixture, the dialysis tube [cellulose membrane avg. flat width 10 mm (0.4 in.), Sigma] was placed in boiling water for 30 min and rinsed with a copious amount of water. Liposome mixtures were transferred to dialysis tubing and both ends were tied. This was added against 7 ml of PBS (pH 7.4) [Kriwet and Müller-Goymann, 1995], for removal of non-encapsulated drug for 1 h.

2.6 Drug release experiment

152 The 7 ml of PBS were removed and replace with fresh PBS and drug release profiles was
153 analysed by extraction of 500 µL aliquots of the immersion medium at intervals of 30 min, 1,
154 2, 3, 4, 15, 24, 48, 72 h and 8, 16 days at 37 ºC. Each time the extracted volume was replaced
155 with fresh PBS pre-equilibrated at 37°C making it possible to determine diffusion parameters.
156 The amount of drug released at each time point was determined by UV-Vis using a Varian 50
157 bio UV-visible spectrophotometer at room temperature. The concentration of the drug released
158 from the dialysis tube was determined using a calibration curve of the pure drugs in PBS
159 solutions at the wavelength where showed the maximum absorbance (AT - 275 nm [Lalitha et
160 al., 2013] and Q – 330 nm [Frosch et al., 2007]). The absorbance was converted into percentage
161 release using a standard curve and experiments were performed in triplicates in order to ensure
162 accuracy.
163
164 2.7 Data fitting and Mathematical Model
165 A previously studied mathematical model was used with the results obtained from this study
166 [Peppas and Sahlin, 1989; Joguparthi et al., 2008]. The equation considered for the fitting
167 model was:

168 $$\frac{Mt}{M\infty} = k1.t^m + k2t^{2m} \qquad (1)$$

169 where t represents time, and $k1$, $k2$ and m are constants. $\frac{Mt}{M\infty}$ represents the Fickian diffusional
170 contribution considering the amount of drug released at time t and infinite time. These
171 parameters were used as the initial input in Igor Pro 6.34A in order to refine estimations using
172 an optimization method. Several assumptions were made in order to obtain the mathematical
173 model. Some of the assumptions were: the analysis of the data was based on one-dimensional
174 diffusion; the suspended drug is in a fine state, so particles are much smaller in diameter than
175 the thickness of the system; the diffusivity of the drug is constant; perfect sink conditions were

maintained during drug release experiment; the appearance of drug in the aqueous buffer is a result of the diffusion of the nanoparticles followed by diffusion across the dialysis membrane, although being generally treated as a first order process.

2.7 Statistical analysis

All experiments were performed in triplicates with calculation of means and standard deviations. Two-way analysis of variance (ANOVA) was used for multiple comparisons along with Tukey's multiple comparing test, followed by T-test to access statistical significance for paired comparisons. Significance was acknowledged for p values lower than 0.05. All calculations were made in GraphPad Prism version 6.0 (GraphPad Software Inc., La Jolla, CA).

3. Results and Discussion

3.1 Preparation of Liposomes at different FRR and TFR values

Different TFR and FRR were investigated. Lower TFR and FRR produce larger liposomes (Fig. 3). The combination between the decrease of liposome size due to increase of FRR confirms previous studies in the literature [Jahn et al., 2010; Kastner et al., 2014, 2015]. Although no significant differences were detected in mean size distribution of particles manufactured from 1 to 6 and 6 to 20 ml min^{-1}. Particles fabricated at 20 ml min^{-1} are smaller than the ones obtained at 1 ml min^{-1}. Furthermore, particles formed with 1:1 lipid/cholesterol ratios were smaller. In Fig. 4 the distribution of particle sizes for different TFR and FRR can be observed. For example when comparing the DMPC and DSPC formulations prepared at FRR 1 of ~200 nm, sizes of 137 nm and 98 nm where obtained for formulations prepared from 1:1 DMPC at TFR20 and FRR of 3:1 and 5:1 respectively. For 1:1 DSPC formulations prepared at TFR20 and FRR of 3:1 and 5:1 values of 85 nm and 76 nm respectively. This occurs since the fluid mixing is much faster, thus shear stress forces increase, which leads to the assembling

of smaller particles. Although some literature states that TFR does not significantly influence mean particle size [Jahn et al., 2007; Kastner et al., 2014, 2015], this study shows that TFR impact on particle size can be seen for higher values as 6 and 20 ml min^{-1}. When comparing the formulations with different lipid to CH ratios, for both DMPC and DSPC 2:1 formulations (Fig. 3b and 3d) presented the higher size values, such as 729 nm for 2:1 DMPC TFR1 FRR 3:1, 549 nm 2:1 DMPC TFR1 FRR 5:1, 1043 nm for 2:1 DSPC TFR1 FRR 3:1 and 375 nm for 2:1 DSPC TFR1 FRR 5:1 (Fig. 3). Overall 1:1 liposome formulations for both DMPC and DSPC, presented lower mean size and lower PDI values. For the 1:1 DMPC and DSPC formulations, although differences in size were not significant, TFR of 6 and 20 mL ml^{-1}, and FRR of 5:1 presented the smaller size vesicles. The size of liposomes produced out of 1:1 lipid/cholesterol ratio ranged from ~70 nm to ~200 nm. The highest values of mean size are seen for 2:1 DMPC and 2:1 DSPC were the liposomes were formed at lower TFR (1) and FRR (3:1). When compared with our previous study [Briuglia et al., 2015], microfluidic allows the production of liposomes with smaller mean particle size by altering TFR and FRR. The zeta potential of the liposomes formed did not suffer significantly alterations despite differences in flow rates. Ratios with the liposomes had a negative zeta potential of around 0 and -10 mV.

3.2 Effect of Manufacturing on stability and encapsulation efficacy

According to our stability tests, following microfluidics procedure, the more stable liposomes result with 1:1 lipid/cholesterol ratio. This is the first major difference compared to our previous study [Briuglia et al., 2015], where the best formulation was 2:1. The formulations prepared at low TFR (1 ml min^{-1}) present high standard deviations for the particle size distribution. Our results show that the more stable formulations were DMPC/CH 1:1 TFR20 ml min^{-1} FR5:1, DMPC/CH 2:1 TFR6 ml min^{-1} 5:1, DSPC/CH 1:1 TFR6 ml min^{-1} 3:1, and DSPC/CH 2:1 TFR20 ml min^{-1} 5:1. These results are accordingly to literature, which states that

a 50 % mol/mol ratio for lipid and cholesterol is ideal for liposome stability [Gregoriadis and Davis, 1979; Kirby et al., 1980]. Additionally, liposome formulations became more stable with the increase of TFR (6 and 20 ml ml^{-1}) and with the increase of FRR (5:1). The graphs obtained from the stability studies of the most stable formulations can be found in Fig. 4. These were the ones used in further studies of AFM, IR, and drug release.

Encapsulation efficiency (EE) values are very important as they give an insight on whether the production method can be applicable to the industrial background or not. EE data can be found on Table 1. Values of EE proved to be higher for ATL formulations. These results are in accordance to our previous study [Briuglia et al., 2015], where ATL showed overall higher values of encapsulation efficiency than Q, even though they were produced by a different method.

Hydrophilic and hydrophobic drugs will be loaded into the liposomes on different sites. Entrapment of hydrophilic molecules occurs in the aqueous compartments of the vesicle while hydrophobic drugs have higher affinity to the lipid bilayers of the vesicle [Kulkarni et al., 1995]. Hydrophilic encapsulation for example is also influenced by liposome size, being that encapsulation efficiencies achieved are higher for large unilamellar vesicles. Additionally, charged vesicles improve hydrophilic loading [Kulkarni et al., 1995]. Although loading values of hydrophobic molecules are not majorly affected by liposome size, and multilamellar vesicles seem to be the most suitable [Kulkarni et al., 1995]. Furthermore, the characteristics of lipids used during manufacturing and presence of cholesterol are key players for hydrophobic encapsulation [Kulkarni et al., 1995]. Higher CH concentrations will have a decreasing effect on membrane permeability. Hydrophobic loading will be highly dependent on lipid bilayer characteristics, and higher results seem to be achieved for fluid membranes [Kulkarni et al., 1995]. Furthermore, CH seems to present a competitive action with the hydrophobic drug during the assembly and encapsulation for packing space in the lipid bilayer

[Ali et al., 2010]. Formulations that present lower CH contents were expected to show better encapsulation efficacy. This did not occur for the incorporation of quinine in the 2:1 DMPC formulation prepared at TFR 6 ml ml^{-1} FR 5:1 when compared to 1:1 DMPC prepared at TFR 20 ml ml^{-1} and FRR of 5:1. This may indicate that a higher mixing rate could cause better encapsulation. Studies show that liposome size, and lipid size and composition, play a crucial part in dictating drug release profiles and encapsulation efficiency [Betageri and Parsons, 1992]. Manufacturing methods may also influence EE [Kulkarni et al., 1995]. EE values of the two drugs were very similar to our previous study where film hydration method was used [Briuglia et al., 2015]. In general, the results obtained from this study indicate that the microfluidic manufacturing process allows for high EE results of ~100 % for ATL and of ~70 % for Q. Also, this study shows that microfluidic technique is a faster method of encapsulating drugs into liposomal products. This was to be expected since recent studies [Kastner et al., 2014, 2015], also using the Nanoassemblr, describe the ability of merging liposome manufacturing and drug encapsulation in a single process step, as well as flexibility and ease of applying lab-on-a-chip technique. These characteristics would have great impact in industry [Kastner et al., 2014, 2015].

3.3 AFM

Atomic force microscopy is a fast and easy to perform method, which allows to evaluate liposomes morphology. The most stable formulations that were mentioned in the previous section (DMPC/CH 1:1 TFR20 ml min^{-1} FR5:1, DMPC/CH 2:1 TFR6 ml min^{-1} 5:1, DSPC/CH 1:1 TFR6 ml min^{-1}3:1, and DSPC/CH 2:1 TFR20 ml min^{-1} 5:1) were used for the AFM studies. AFM results are presented in figure 5.

The diameter acquired by AFM measurements is comparable to DLS acquired data, where some differences can be spotted. The liposomes present sizes of around 200-300 nm among

the different formulations which can be seen in Table 2. Differences can be seen when compared with DLS size results. Reasoning behind these can be liposomes composition between formulations, causing changes in the structures left after they dry and collapse on the mica surface, and also deformations caused by the tip of AFM probe [Ruozi et al., 2007]. Despite this, results obtained are concordant with literature that describes liposome images as asymmetrical flattened structures described as planar vesicles [Ruozi et al., 2007]. These are also according to our previous study, where presence of cholesterol improved the shape of liposomes by stabilizing them [Briuglia et al., 2015].

3.4 FT-IR

IR spectroscopy is a complex method, which is especially useful since the resulting spectrum acts as a fingerprint for compounds. This analysis was performed on the four formulations that were the most stable (DMPC/CH 1:1 TFR20 ml min^{-1} FR5:1, DMPC/CH 2:1 TFR6 ml min^{-1} 5:1, DSPC/CH 1:1 TFR6 ml min^{-1}3:1, and DSPC/CH 2:1 TFR20 ml min^{-1} 5:1). Medium intensity bands near 3000 cm^{-1} DMPC and DSPC spectrum represent C-H single-bond stretching motions (Fig. 6). C-H scissoring or bend can be seen at 1330-1500 cm^{-1}. The other important bond present occurs at 1680 to 1750 cm^{-1} and represents the carbonyl group of the ester bond [Larkin, 2011]. The IR spectrum of the different ratios of lipids and CH can be seen in Fig. 3. The major difference between both DMPC and DSPC spectrum, comparing the different ratios, is the intensity of the peaks. The spectrums of the 2:1 lipid ratios show strongest peaks. When CH is present at higher concentrations, as it happens in the 1:1 formulation, it interacts with the phospholipids provoking steric hindrance that ultimately results in weaker peaks. This is more noticeable in the DMPC spectrums. Such results are in accordance to our previous results [Briuglia et al., 2015], using the film hydration method. This indicates that the

microfluidic technique does not alter the composition of the lipids not the way in which CH interacts with the phospholipids.

3.5 Drug release

Drug release studies are mainly influenced by liposome size, lipid composition, and lipids chain length. The drug release profile will depend on where the drug is accommodated within the liposome. A hydrophilic drug will be dissolved in the aqueous space inside the vesicles and hydrophobic compounds are accommodated within the lipid bilayer. Q and AT drug release profile graph can be seen in Fig. 7. According with literature [Hua, 2014], all of the different formulations showed an initial burst of drug release. AT showed similar release profiles for the different formulations. In our previous paper, each time liposomes were formulated by hydration method, AT release resulted in faster release than Q.

In this study, there is not a distinct behaviour between AT and Q. AT presents a faster release profile for DMPC formulations. On the contrary, Q shows a faster release for DSPC formulations, especially for 1:1 DSPC that was prepared at TFR of 20 ml min^{-1} and FRR 5:1. This may be related to the fact that DSPC has an increased lipid chain length, and there seems to be a tendency for an increase of loading and encapsulation efficiency with increasing lipid chain length [Mohammed et al., 2004]. Furthermore, different values of TFR and FRR can form liposomes slightly different structured compared to the formulations through film hydration method. For example, if the liposomes produced with microfluidics are unilamellar vesicles, this leads to higher stability and encapsulation of hydrophilic vesicles. Consequently, release profile of ATL would be slower. Since hydrophobic molecules have higher affinity for multilamellar vesicles, Q encapsulation values achieved would be lower, ultimately leading to a faster release of the drug.

Formulations which contained 2:1 lipid/cholesterol contents, presented faster release profiles with higher maximum releases, when compared with formulations with 1:1 lipid/cholesterol ratio. According to previous studies with hydrophobic drugs, higher retention rates are seen with the increase of CH content in the formulation. As CH is present in increasing contents, it stabilizes liposomes but it obstructs the leakage of hydrophobic drugs [Ali et al., 2010]. Despite this, 1:1 DSPC formulation encapsulated with Q, showed the fastest release.

From these results, we can see that microfluidic manufacturing may alter the way drugs are loaded within the liposomes formed, ultimately causing changes in release profile of a specific drug. This method allows different outcome possibilities accordingly to the lipid and drug in question. When comparing these results with our previous study, we can see that altering microfluidic parameters influences the drugs interaction with the liposomes, making it possible to achieve faster release profiles for Q.

The developed fitting model, based on Eq. 1, can be seen in Fig. 8 and values for the constants of $k1$, $k2$ and m can be found in Table 3. From Fig. 8, a good correlation between drug release profiles obtained in this study and the predicted values can be observed. These results validate the obtained mathematical model.

4. Conclusions

In this study, we showed the applicability of microfluidic manufacturing method as a simpler and faster way for liposomes production. Liposomes can be adjusted and manipulated by changing different parameters during assembly, such as TFR and FRR. It is possible to obtain smaller and more stable liposomes increasing or reducing the TFR or the FRR. The versatility of microfluidic is very promising and it provides a suitable alternative method to film hydration. Microfluidic simplifies the encapsulation step, without losing encapsulation efficiency, making it much faster than traditional manufacturing methods. Moreover, by

microfluidics, the scale-up for particle production will be possible by manufacturing a scale-up system that can be mainly used for clinical-size batches, with all-in-one scale-up system and not by having multiple steps as in film hydration method. However, the production of large scale (industrial) materials using current microfluidic technologies can be a challenge (Carugo et al., 2016).

Acknowledgements

The authors would like to thank the EPSRC Centre in Continuous Manufacturing and Crystallisation (EPSRC) for access to equipment and the ERASMUS programme for the mobile scholarship.

356 **References**

357 Ali, M. H., Kirby, D. J., Mohammed, A. R., and Perrie, Y., 2010. Solubilisation of drugs
358 within liposomal bilayers: Alternatives to cholesterol as a membrane stabilising agent. J.
359 Pharm. Pharmacol. 62, 1646–1655.

360 Belliveau, N. M., Huft, J., Lin, P. J., Chen, S., Leung, A. K., Leaver, T. J., Wild, A. W., Lee,
361 J. B., Taylor, R. J., Tam, Y. K., Hansen, C. L., and Cullis, P. R., 2012. Microfluidic
362 Synthesis of Highly Potent Limit-size Lipid Nanoparticles for In Vivo Delivery of
363 siRNA. Mol. Ther. — Nucleic Acids 1, e37.

364 Betageri, G. V., and Parsons, D. L., 1992. Drug encapsulation and release from multilamellar
365 and unilamellar liposomes. Int. J. Pharm. 81, 235–241.

366 Briuglia, M.-L., Rotella, C., McFarlane, A., and Lamprou, D. a., 2015. Influence of
367 cholesterol on liposome stability and on in vitro drug release. Drug Deliv. Transl. Res.
368 231–242.

369 Carugo, D., Bottaro, E., Owen, J., Stride, E., and Nastruzzi, C, 2016. Liposome production by
370 microfluidics: potential and limiting factors. Sci. Rep. 6, Article number: 25876,
371 doi:10.1038/srep25876

372 Frosch, T., Schmitt, M., and Popp, J., 2007. In situ UV resonance Raman micro-
373 spectroscopic localization of the antimalarial quinine in cinchona bark. J. Phys. Chem. B
374 111, 4171–4177.

375 Gregoriadis, G., and Davis, C., 1979. Stability of liposomes invivo and invitro is promoted by
376 their cholesterol content and the presence of blood cells. Biochem. Biophys. Res.
377 Commun. 89, 1287–1293.

Heurtault, B., 2003. Physico-chemical stability of colloidal lipid particles. Biomaterials 24, 4283–4300.

Hua, S., 2014. Comparison of in vitro dialysis release methods of loperamide-encapsulated liposomal gel for topical drug delivery. Int. J. Nanomedicine 9, 735–744.

Immordino, M. L., Dosio, F., and Cattel, L., 2006. Stealth liposomes: Review of the basic science, rationale, and clinical applications, existing and potential. Int. J. Nanomedicine 1, 297–315.

Jahn, A., Vreeland, W. N., Gaitan, M., and Locascio, L. E., 2004. Controlled Vesicle Self-Assembly in Microfluidic Channels with Hydrodynamic Focusing. J. Am. Chem. Soc. 126, 2674–2675.

Jahn, A., Vreeland, W. N., Devoe, D. L., Locascio, L. E., and Gaitan, M., 2007. Microfluidic directed formation of liposomes of controlled size. Langmuir 23, 6289–6293.

Jahn, A., Stavis, S. M., Hong, J. S., Vreeland, W. N., Devoe, D. L., and Gaitan, M., 2010. Microfluidic mixing and the formation of nanoscale lipid vesicles. ACS Nano 4, 2077–2087.

Joguparthi, V., Xiang, T., and Anderson, B. D., 2008. Liposome transport of hydrophobic drugs: Gel phase lipid bilayer permeability and partitioning of the lactone form of a hydrophobic camptothecin, DB-67. J. Pharm. Sci. 97, 400–420.

Kastner, E., Kaur, R., Lowry, D., Moghaddam, B., Wilkinson, A., and Perrie, Y., 2014. High-throughput manufacturing of size-tuned liposomes by a new microfluidics method using enhanced statistical tools for characterization. Int. J. Pharm. 477, 361–368.

Kastner, E., Verma, V., Lowry, D., and Perrie, Y., 2015. Microfluidic-controlled manufacture

of liposomes for the solubilisation of a poorly water soluble drug. Int. J. Pharm. 485, 122–30.

Kirby, C., Clarke, J., and Gregoriadis, G., 1980. Effect of the cholesterol content of small unilamellar liposomes on their stability in vivo and in vitro. Biochem. J. 186, 591–598.

Kreuter, J., 1994. Colloidal Drug Delivery Systems. - Taylor & Francis.

Kriwet, K., and Müller-Goymann, C. C., 1995. Diclofenac release from phospholipid drug systems and permeation through excised human stratum corneum. Int. J. Pharm. 125, 231–242.

Kulkarni, S. B., Betageri, G. V, and Singh, M., 1995. Factors affecting microencapsulation of drugs in liposomes. J. Microencapsul. 12, 229–246.

Lalitha, K. V., Kiranjyothi, R., and Padma, B., 2013. Uv Spectrophotometric Method Development and Validation for the Determination of Atenolol and Losartan Potassium By Q-Analysis. Int. Bull. Drug Res. 3, 54–62.

Larkin, P., 2011. Infrared and Raman Spectroscopy; Principles and Spectral Interpretation. - Elsevier Science.

Modi, S., and Anderson, B. D., 2013. Determination of drug release kinetics from nanoparticles: overcoming pitfalls of the dynamic dialysis method. Mol. Pharm. 10, 3076–3089.

Mohammed, A. R., Weston, N., Coombes, A. G. A., Fitzgerald, M., and Perrie, Y., 2004. Liposome formulation of poorly water soluble drugs: Optimisation of drug loading and ESEM analysis of stability. Int. J. Pharm. 285, 23–34.

Pattni, B. S., Chupin, V. V., and Torchilin, V. P., 2015. New Developments in Liposomal

422 Drug Delivery. Chem. Rev. 150526165100008.

423 Peppas, N. A., and Sahlin, J. J., 1989. A simple equation for the description of solute release.
424 III. Coupling of diffusion and relaxation. Int. J. Pharm. 57, 169–172.

425 Ruozi, B., Tosi, G., Leo, E., and Vandelli, M. A., 2007. Application of atomic force
426 microscopy to characterize liposomes as drug and gene carriers. Talanta 73, 12–22.

427 Squires, T. M., and Quake, S. R., 2005. Microfluidics Fluid physics at the nanoliter. in press.

428 Whitesides, G. M., 2006. The origins and the future of microfluidics. Nature 442, 368–73.

429 Yadav, A. V., Murthy, M. S., Shete, A. S., and Sakhare, S., 2011. Stability aspects of
430 liposomes. Indian J. Pharm. Educ. Res. 45, 402–413.

431

Figures legend:

Fig. 1 Representation of microfluidic chip for Nanoassemblr.

Fig. 2 Chemical structures of the compounds used: (a) 2-dimyristoyl-sn-glycero-3-phosphocholine (DMPC), (b) cholesterol (CH), (c) 1,2-distearoyl-sn-glycero-3-phosphocholine (DSPC), (d) atenolol (ATL) and (e) quinine (Q).

Fig. 3 Average particle size of all the formulations under different TFR and FRR, (a) DMPC/CH 1:1 , (b) DMPC/CH 2:1, (c) DSPC/CH 1:1, and (d) DSPC/CH 2:1, where $p \leq 0.05$ comparing with week 1;** - $p \leq 0.01$ comparing with week 1;*** - $p \leq 0.001$ comparing with week 1;**** - $p \leq 0.0001$ comparing with week 1; # - $p \leq 0.05$ comparing with week 2; ## - $p \leq 0.01$ comparing with week 2; ### - $p \leq 0.001$ comparing with week 2; #### - $p \leq 0.0001$ comparing with week 2; + - $p \leq 0.05$ comparing with week 3; ++ - $p \leq 0.01$ comparing with week 3; +++ - $p \leq 0.001$ comparing with week 3; ++++ - $p \leq 0.0001$ comparing with week 3.

Fig. 4 Average particle size of the most stable formulations from week 1 to week 3 (* - $p \leq 0.05$ comparing with TFR1 FRR 3:1;** - $p \leq 0.01$ comparing with TFR1 FRR 3:1;*** - $p \leq$ comparing with TFR1 FRR 3:1;**** - $p \leq 0.0001$ comparing with TFR1 FRR 3:1; # - $p \leq 0.05$ comparing with TFR1 FRR 5:1; ## - $p \leq 0.01$ comparing with TFR1 FRR 5:1; ### - $p \leq 0.001$ comparing with TFR1 FRR 5:1; #### - $p \leq 0.0001$ comparing with TFR1 FRR 5:1; º - $p \leq 0.05$ comparing with TFR6 FRR 3:1; ºº - $p \leq 0.01$ comparing with TFR6 FRR 3:1; ººº - $p \leq 0.001$ comparing with TFR6 FRR 3:1; ºººº - $p \leq 0.0001$ comparing with TFR6 FRR 3:1; ‘ - $p \leq 0.05$ comparing with TFR6 FRR 5:1; ‘’ - $p \leq 0.01$ comparing with TFR6 FRR 5:1; ‘’’ - $p \leq 0.001$ comparing with TFR6 FRR 5:1; ‘’’’ - $p \leq 0.0001$ comparing with TFR6 FRR 5:1; x - $p \leq 0.05$ comparing with TFR20 FRR 3:1; xx - $p \leq 0.01$ comparing with TFR20 FRR 3:1; xxx - $p \leq$ 0.001 comparing with TFR20 FRR 3:1; xxxx - $p \leq 0.0001$ comparing with TFR20 FRR 3:1); red lines represent results at 4ºC and blue dotted lines represent results at 37ºC.

456 **Fig. 5** FTIR spectra of (a) DMPC/CH 1:1 TFR20 ml min^{-1} FR5:1, (b) DMPC/CH 2:1 TFR6 ml

457 min^{-1} 5:1, (c) DSPC/CH 1:1 TFR6 ml min^{-1} 3:1, and (d) DSPC/CH 2:1 TFR20 ml min^{-1} 5:1

458 **Fig. 6** AFM images of (a) DMPC/CH 1:1 TFR20 ml min^{-1} FR5:1, (b) DMPC/CH 2:1 TFR6 ml

459 min^{-1} 5:1, (c) DSPC/CH 1:1 TFR6 ml min^{-1}3:1, and (d) DSPC/CH 2:1 TFR20 ml min^{-1} 5:1

460 **Fig. 7** Drug release graphs of (a) quinine, and (b) atenolol.

461 **Fig. 8** Fitting model obtained from drug release data of (a) quinine, and (b) atenolol.

462 **Table 1.**

Lipid/cholesterol ratio	TFR	FR	Atenolol (%EE)	Quinine (%EE)
DMPC 1:1	20	5:1	99.95	71.88
DMPC 2:1	6	5:1	99.95	51.54
DSPC 1:1	6	3:1	99.96	75.60
DSPC 2:1	20	5:1	99.95	77.81

463

464 **Description:**

465 Table 1 shows results of Encapsulation Efficiency (%EE) for Atenolol and Quinine using the

466 best formulations obtained from previous experiences.

467 **Table 2.**

Lipid/cholesterol ratio	TFR	FR	Size/nm
DMPC 1:1	20	5:1	363.67± 39.78
DMPC 2:1	6	5:1	217.83± 18.33
DSPC 1:1	6	3:1	251.83± 46.55
DSPC 2:1	20	5:1	266.83± 48.43

468

469 **Description:**

470 Table 2 shows liposome sizes for AFM images.

471 **Table 3.**

472 **FITTING MODEL**

473 (a)

(a)	1:1 DMPC TFR20 FRR 5:1 Atenolol	2:1 DMPC TFR6 FRR 5:1 Atenolol	1:1 DSPC TFR6 FRR 3:1 Atenolol	2:1 DSPC TFR20 FRR 5:1 Atenolol
k_1	10.832 ± 0.973	15.528 ± 1.45	14.883 ± 1.23	12.747 ± 0.885
k_2	-0.51233 ± 0.995	-0.91178 ± 0.713	-1.1181 ± 0.185	-0.24065 ± 1.01
m	0.21311 ± 0.0669	0.24234 ± 0.0599	0.30372 ± 0.0297	0.23711 ± 0.056
(b)				
k_1	2.4543 ± 0.614	11.748 ± 2.12	12.507 ± 1.9	9.9142 ± 1.91
k_2	-0.094561 ± 0.0492	-0.73843 ± 0.288	-0.48886 ± 0.152	-0.3902 ± 0.156
m	0.45703 ± 0.0666	0.3952 ± 0.0481	0.44776 ± 0.0413	0.45255 ± 0.0515

474

475 **Description:**

476 Table 2 Values of the fitting constants: $k1$, $k2$ and m for (a) atenolol and (b) quinine.

477

478 **Figure 1.**

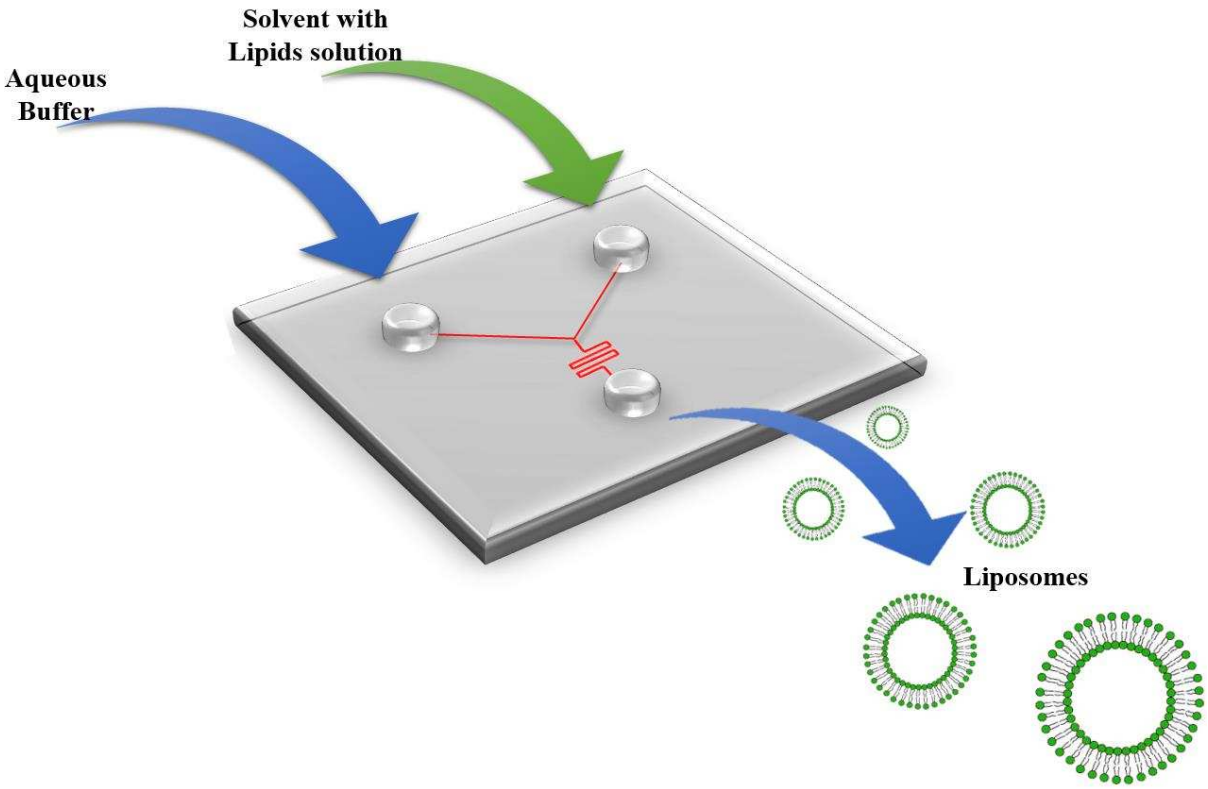

479

480

481 **Figure 2.**

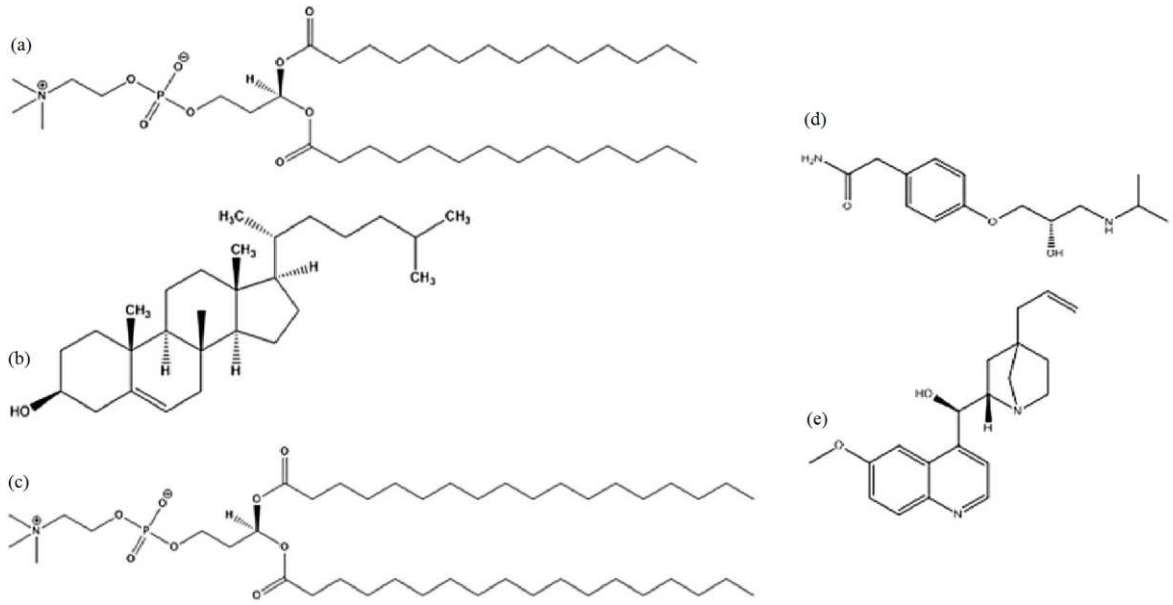

482

483

484 **Figure 3.**

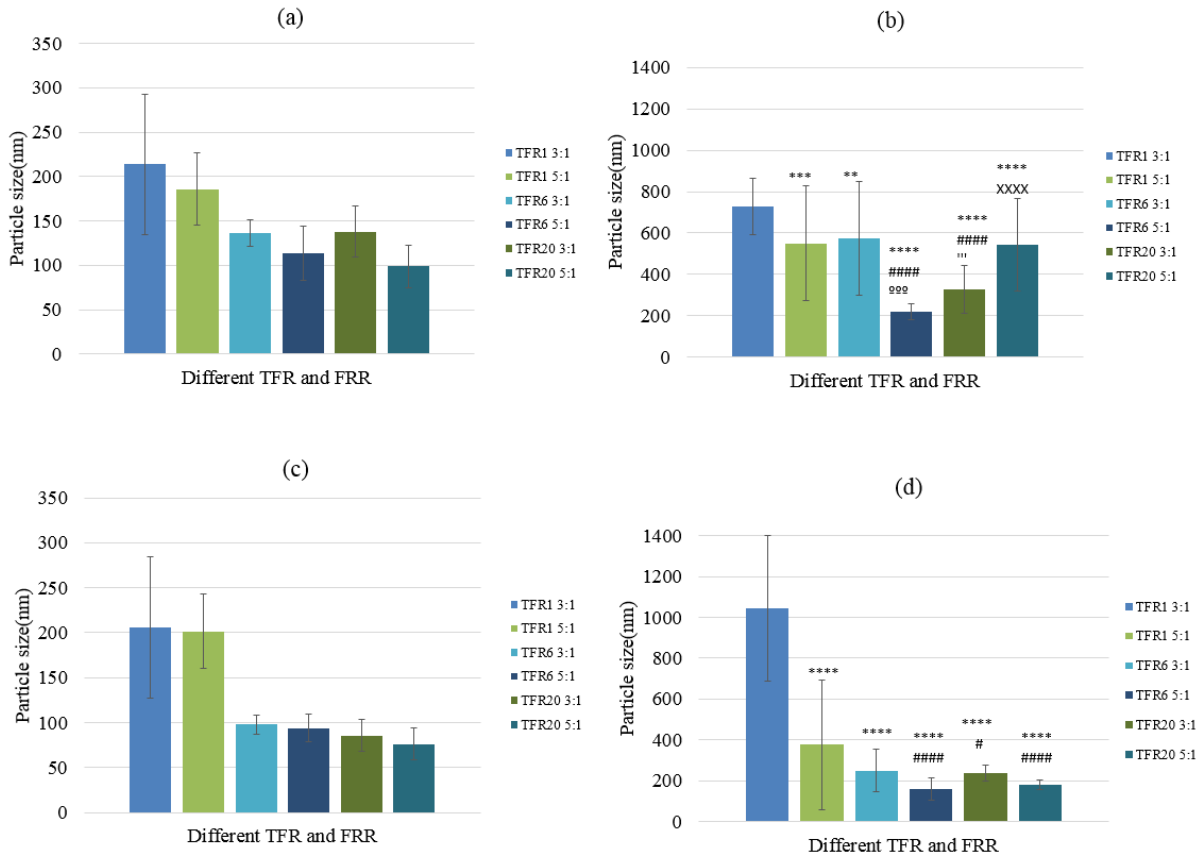

485

486

487 **Figure 4.**

488

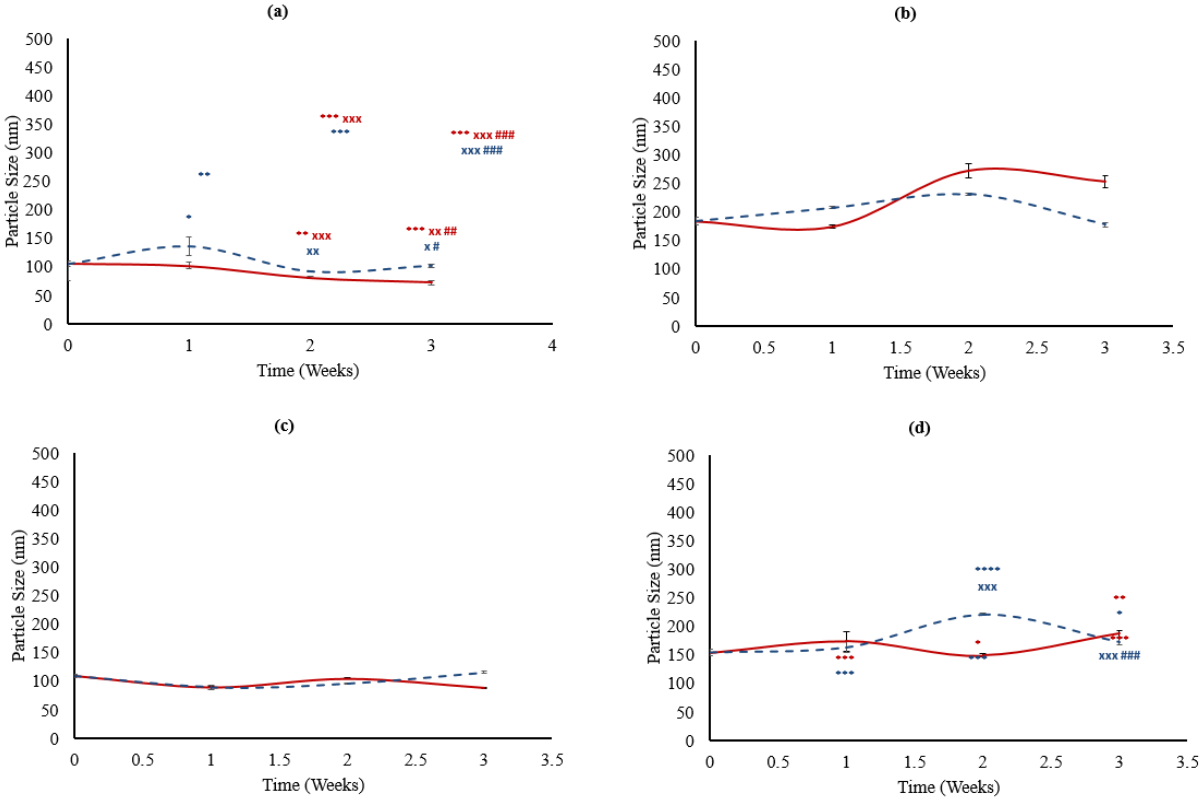

Figure 5.

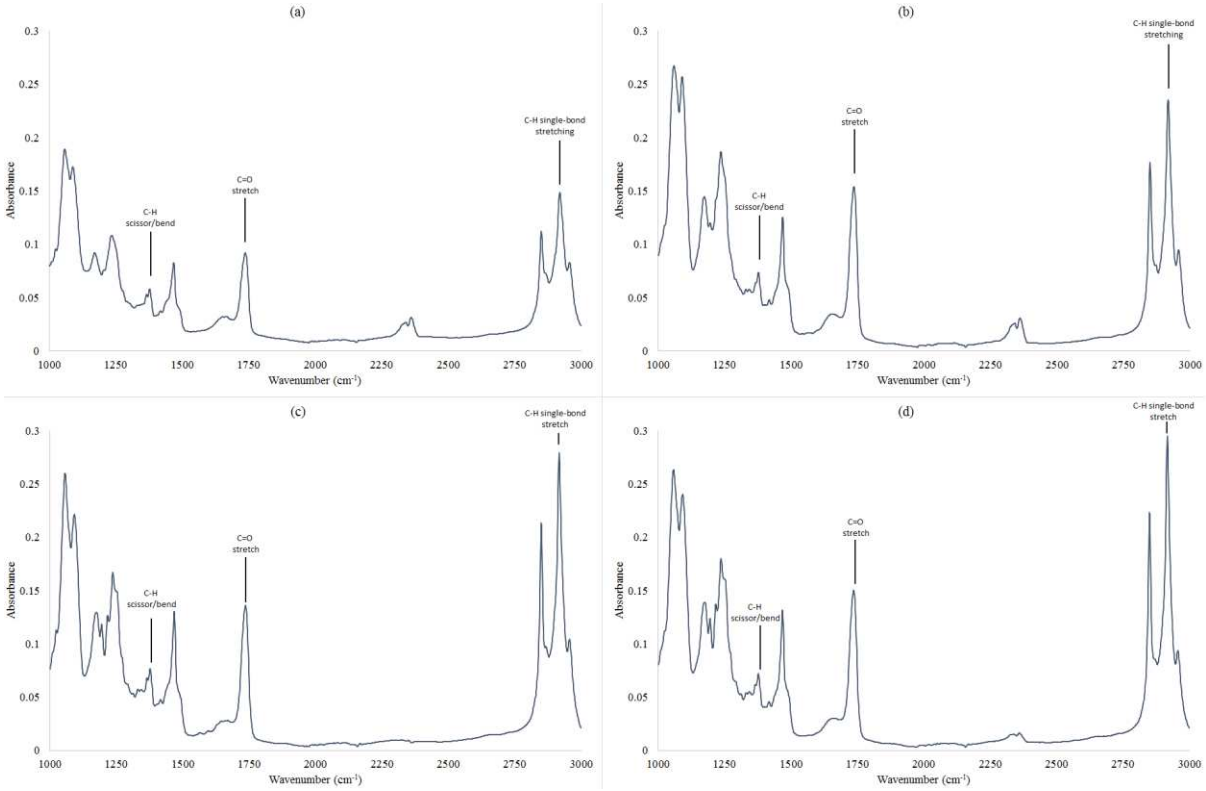
(a)
(b)
(c)
(d)
Absorbance
Wavenumber (cm-1)
C-H scissor/bend
C=O stretch
C-H single-bond stretching
C-H single-bond stretch

493 **Figure 6.**

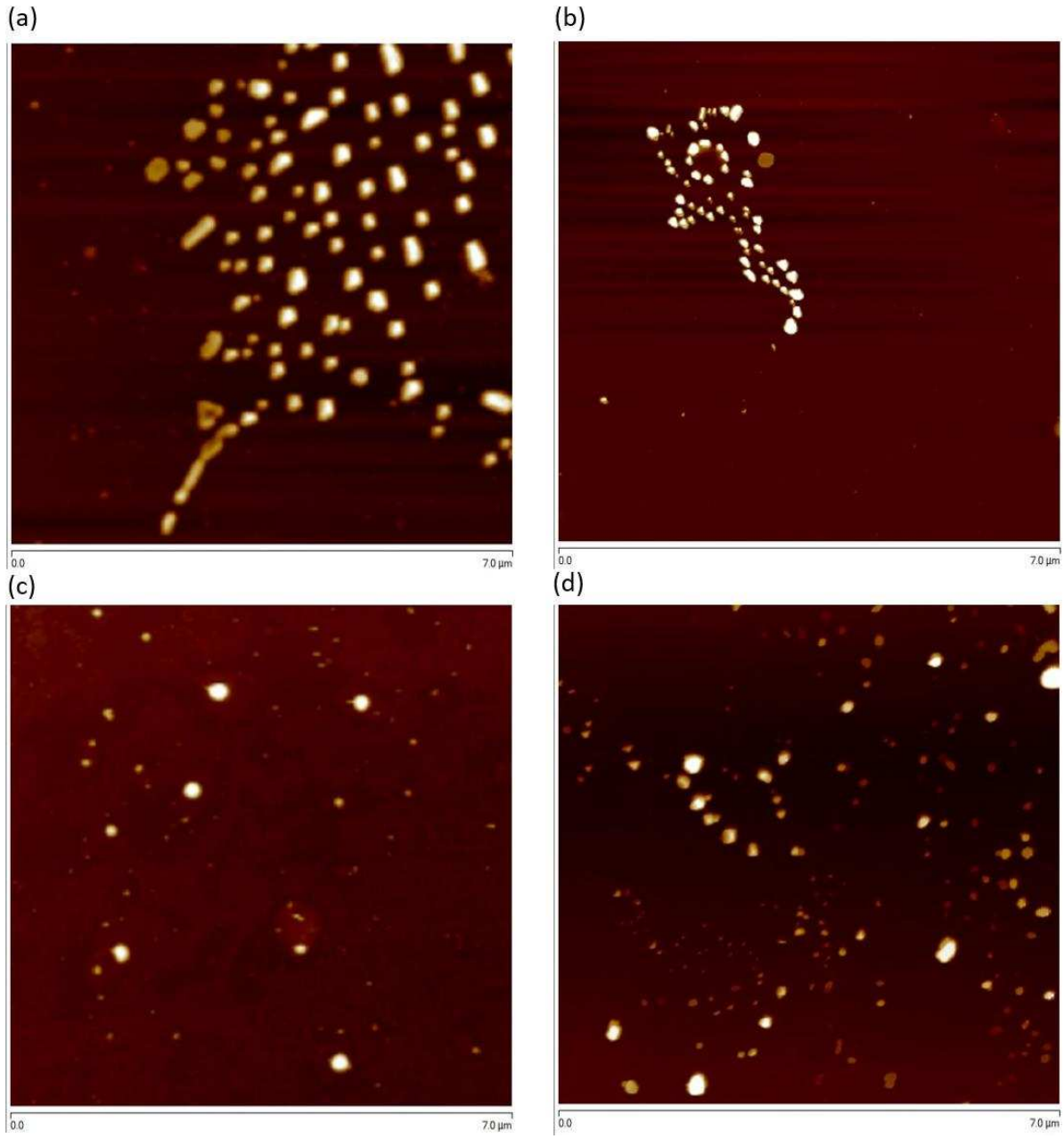

494

495

496 **Figure 7.**

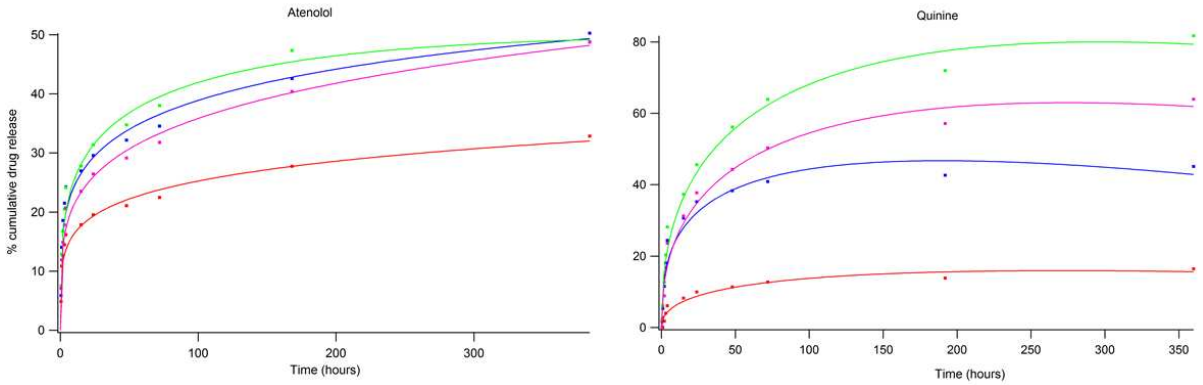

497

498

499 **Figure 8.**

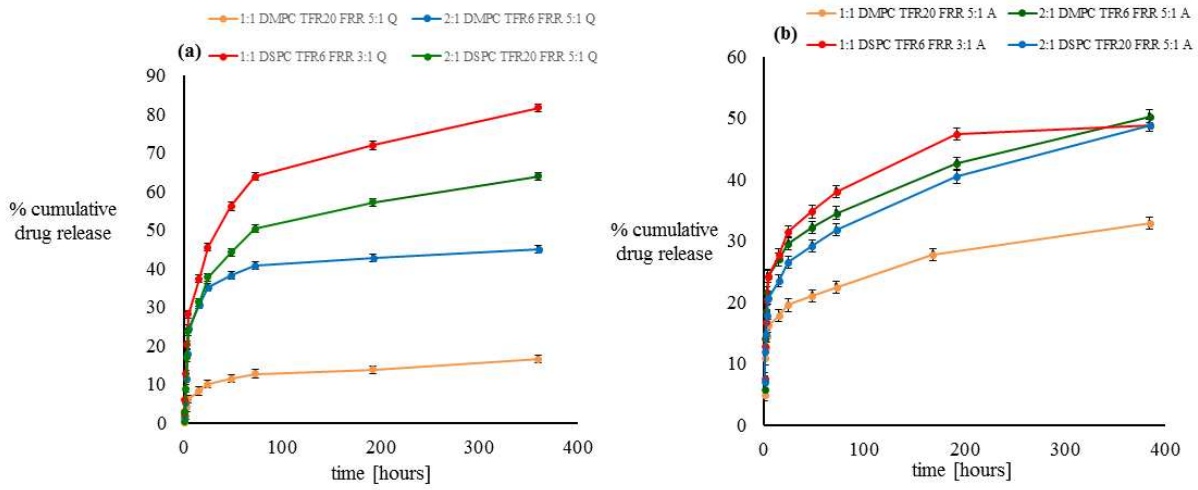

500

501